The EMBO Journal vol.14 no.24 pp.6339–6347, 1995

Changes in network topology during the replication of kinetoplast DNA

Junghuei Chen, Paul T.Englund[1] and Nicholas R.Cozzarelli

Department of Molecular and Cell Biology, University of California, Berkeley, Berkeley, CA 94720 and [1]Department of Biological Chemistry, Johns Hopkins University School of Medicine, Baltimore, MD 21205, USA

Kinetoplast DNA of *Crithidia fasciculata* is a network containing several thousand topologically interlocked DNA minicircles. In the prereplicative Form I network, each of the 5000 minicircles is intact and linked to an average of three neighbors (i.e. the minicircle valence is 3). Replication involves the release of minicircles from the interior of the network, the synthesis of nicked or gapped progeny minicircles and the attachment of the progeny to the network periphery. The ultimate result is a Form II network of 10 000 nicked or gapped minicircles. Our measurements of minicircle valence and density, and the network's surface area, revealed striking changes in network topology during replication. During the S phase, the peripheral newly replicated minicircles have a density twice that of minicircles in Form I networks, which suggests that the valence might be as high as 6. Most of the holes in the central region that occur from the removal of intact minicircles are repaired so that the central density and valence remain the same, as in prereplicative networks. When minicircle replication is complete at the end of the S phase, the isolated network has the surface area of a prereplicative network, despite having twice the number of minicircles. During the G_2 phase, the Form II network undergoes a remodeling in which the area doubles and the valence is reduced to 3. Finally, the interruptions in the minicircles are repaired and the double-sized network splits in two.

Keywords: *Crithidia fasciculata*/DNA topology/kinetoplast DNA/replication

Introduction

Kinetoplast DNA (kDNA) of trypanosomatid mitochondria consists of thousands of DNA rings topologically interlocked into a giant network (reviewed in Ray, 1987; Simpson, 1987; Stuart and Feagin, 1992; Shapiro and Englund, 1995). In *Crithidia fasciculata*, the subject of this study, the network contains ~5000 minicircles of 2.5 kb and 25 maxicircles of ~38.0 kb. In this species, nearly all of the minicircles have the same nucleotide sequence (Sugisaki and Ray, 1987). Isolated *C.fasciculata* networks not undergoing replication are an elliptically shaped 2-D array of interlocked rings, ~10×15 μm in size (Pérez-Morga and Englund, 1993b). Inside the mitochondrial matrix, the network is still a monolayer but is condensed into a disk ~1.0 μm in diameter and 0.4 μm thick (Ferguson *et al.*, 1992).

The kDNA network is the sole genetic material of the trypanosomatid's mitochondrion. Like conventional mitochondrial DNA, the maxicircles encode ribosomal RNAs and several mitochondrial proteins (Simpson, 1987). However, most maxicircle transcripts are processed by extensive editing in which the addition or deletion of uridine residues at multiple specific sites within the transcript creates a functional open reading frame (for reviews, see Stuart and Feagin, 1992; Hajduk *et al.*, 1993; Benne, 1994; Simpson and Maslov, 1994). Both maxicircles and minicircles encode small guide RNAs, which determine the specificity of editing.

The kinetoplast network thus serves a function like that of the nuclear chromosome, except that the genetic elements are held together and compacted by catenation. The challenge is to determine how the network is duplicated and then distributed to the daughter cells. Key features of kDNA replication have been determined (reviewed in Ray, 1987; Shlomai, 1994; Shapiro and Englund, 1995). Before replication begins, all 5000 *C.fasciculata* minicircles are covalently closed; this type of network is called Form I. During the S phase, individual minicircles are released from the network by a type II topoisomerase, and are thought to migrate to one of two complexes of replication proteins situated on opposite edges of the kinetoplast disk (Melendy *et al.*, 1988; Ferguson *et al.*, 1992). Here they replicate as theta structures. The daughter minicircles, which contain nicks and gaps, are reattached in another topoisomerase reaction to the network periphery. Newly attached minicircles are found adjacent to the protein complexes, but eventually they are distributed uniformly around the network periphery (Simpson and Simpson, 1976; Pérez-Morga and Englund, 1993a). To account for this uniform distribution, it has been hypothesized that there is a rotation of the kinetoplast disk relative to the replication complexes (Pérez-Morga and Englund, 1993a).

Because of the peripheral attachment of newly synthesized minicircles, the replicating network develops two zones (Pérez-Morga and Englund, 1993b). The central zone contains covalently closed minicircles that have not been replicated, and the peripheral zone contains nicked or gapped minicircles that have undergone replication. As replication proceeds, the central zone gradually shrinks and the peripheral zone enlarges. When the S phase is complete, the network, termed Form II, has ~10 000 minicircles that are nicked or gapped. Following repair of the nicks and gaps, the duplicated network splits in two (Pérez-Morga and Englund, 1993b). The progeny Form I networks then segregate into the daughter cells during cell division.

Recently we have investigated the topology of

C.fasciculata Form I kDNA networks. We found that minicircles, unlike other naturally occurring circular DNAs, are relaxed rather than negatively supercoiled (Rauch *et al.*, 1993). In addition, each minicircle is linked to its neighbors in the network by a single interlock. We measured the minicircle valence (the average number of minicircles linked to each minicircle in the network) by analyzing the products of a random degradation of the network. We found that the average minicircle valence in a Form I network is 3, and we suggested that the minicircles are organized in a hexagonal array (Chen *et al.*, 1995). This topology is probably the equilibrium position between a balance of forces; the high local minicircle DNA concentration in the kinetoplast favors network formation, but the magnitude of the valence of the network is limited by electrostatic repulsion and DNA rigidity.

In the simplest model for replication the valence remains as 3 during replication, with the newly replicated rings added only to the periphery where the valence shell is incomplete (Cozzarelli, 1993). The result would be a doubling of the network surface area, and topoisomerases would need to act only twice (in the removal and the reattachment of minicircles). However, postreplication Form II networks appear by electron microscopy (EM) to be more densely packed with minicircles than Form I networks (Englund, 1978). This fact suggests that there could be changes in minicircle valence during replication. We therefore investigated the changes in network structure during replication, using new EM methods and measurements of minicircle valence. We found dramatic changes in network topology in both the S and G_2 phases, which led to the proposal of a simple scheme for network replication.

Results

The minicircle density of kDNA networks at different stages of replication

Recently we have demonstrated the utility of modeling kDNA networks using graph diagrams (Chen *et al.*, 1995). Because networks are monolayers of interlocked minicircles, the topology of the network is well represented by planar graphs such as those shown in Figure 1. In these diagrams, each minicircle is represented by a small circle and the topological bonds between minicircles by lines connecting the circles. The model networks differ in valence and the pattern of minicircle interlocking, called tiling. The mean valence for a regular planar graph is between 3 and 6. We have shown that mature Form I networks have an average valence of 3 (n = 3) and that the most likely tiling pattern is the hexagonal pattern shown in Figure 1A (Chen *et al.*, 1995). This is the simplest way to tile a plane.

We distinguish two limiting cases for network topology during kDNA replication. At one extreme, if network topology is unchanged by replication, then the valence remains 3 and the surface area of the isolated network must double. At the opposite extreme, the area is unchanged by replication but the density of minicircles doubles. The replicated network would then have a higher valence because it remains a monolayer (Pérez-Morga and Englund, 1993b; Chen *et al.*, 1995). The planar graph shown in Figure 1C is the only one possible for a valence of 6—a valence twice that of the prereplicative network.

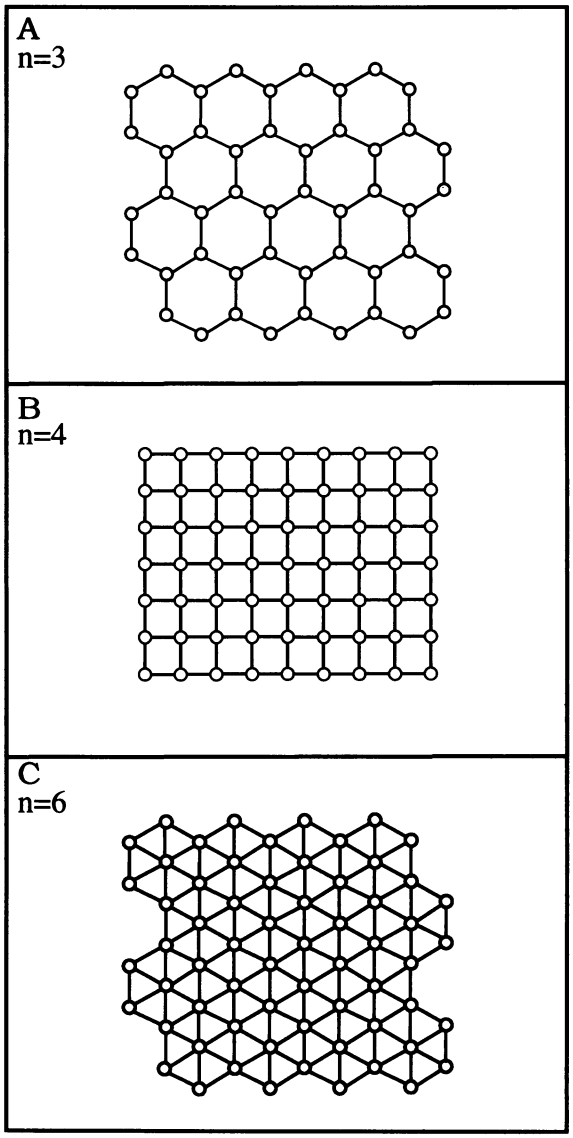

Fig. 1. Models of kDNA networks. Portions of infinite planar graphs that model possible network topologies. The vertices of the graphs (○) represent minicircles, and the edges (—) represent the topological bonds between the circles. n is the valence of the graph, which is the number of edges incident to a vertex or, equivalently, the number of minicircles linked to any minicircle. A tile is defined as the region of a planar graph bounded by edges. The tiles shown are a hexagon (**A**), a square (**B**) or a triangle (**C**). These graphs are univalent (each vertex has the same valence) and regular (all the tiles are the same). These three graphs are the only possible univalent regular planar graphs. We have drawn elsewhere (Chen *et al.*, 1995) the four other univalent planar graphs that have two different tiles; their valence was either 3 or 4. The triangular graph shown in (C) is the only possible regular planar graph for n = 6. Note that this graph can be generated from the graph in (A) merely by adding a vertex in the middle of the hexagonal tile that is joined to all six surrounding vertices.

We have developed a method to analyze network topology that is suitable for all stages of replication. We measured the minicircle planar density by EM in a region of an isolated network. It is a planar or projected density because all height information is lost in the micrographs. Because networks at all stages of replication are monolayers of minicircles, the planar DNA density is a direct

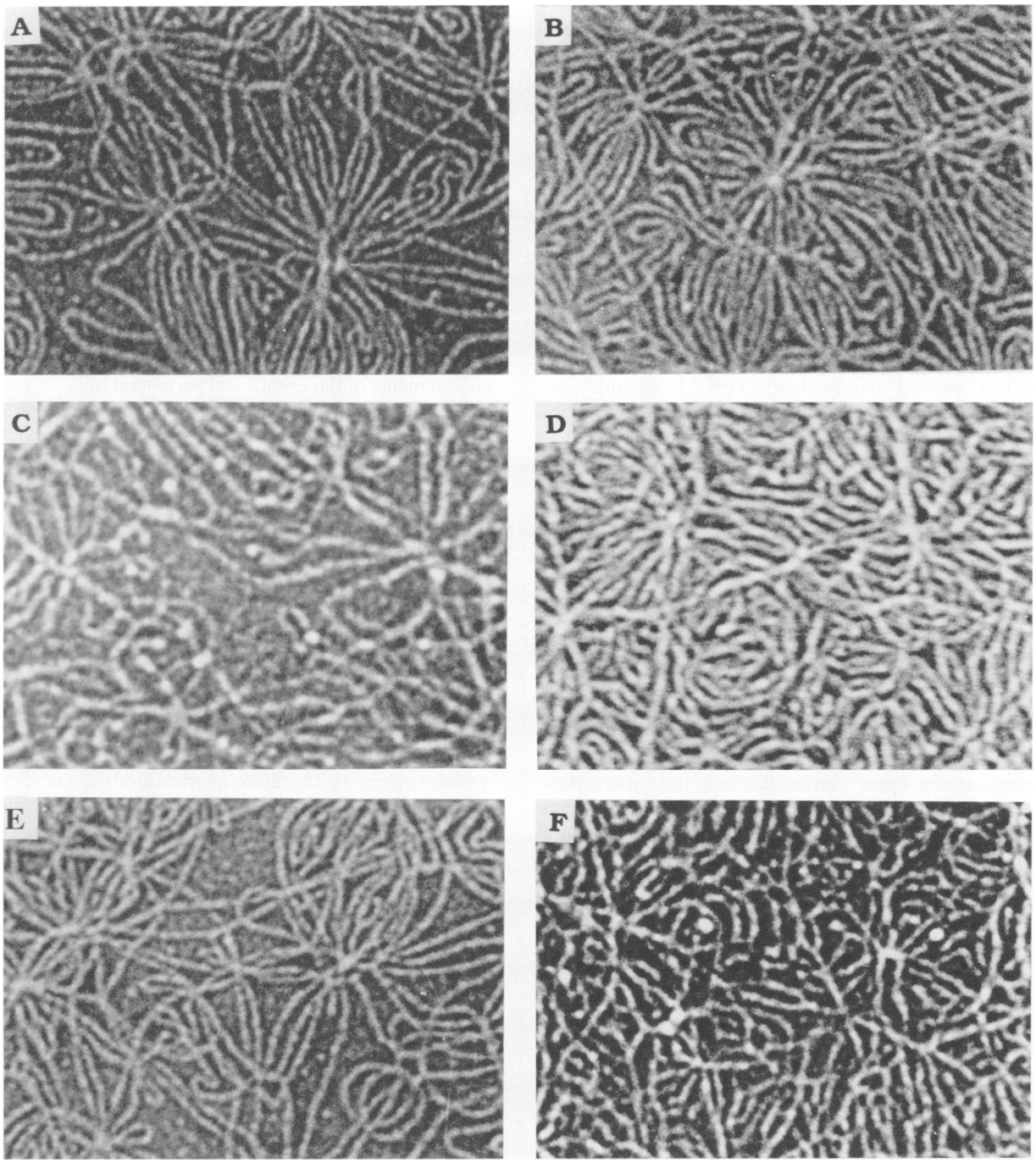

Fig. 2. Enlargements of electron micrographs of portions of networks at three stages of replication. Electron micrographs taken at 5000-fold magnification were enlarged a further 64-fold and the planar density measured as described in the text. (**A**) A Form I network (36 minicircles/μm^2); (**B**) a folded double-thickness region of a Form I network (70 minicircles/μm^2); (**C**) a Form II network in which the DNA density (34 minicircles/μm^2) is about the same as that of an average Form I network; (**D**) a Form II network in which the DNA density (69 minicircles/μm^2) is about twice that of an average Form I network; (**E**) the central zone of a replicating network in which the DNA density (35 minicircles/μm^2) is about the same as an average Form I network; (**F**) the peripheral zone of a replicating network in which the DNA density (75 minicircles/μm^2) is about twice that of an average Form I network. In (F), the DNA was spread for microscopy in the presence of 1 μg/ml ethidium bromide.

measure of the 3-D density of DNA. Thus, the density of an isolated network is an indirect measure of its valence.

We established a calibration for our density determinations by measuring the density of Form I networks whose structure we had determined previously (Chen *et al.*, 1995). We made 64-fold enlargements of segments of electron micrographs of networks, thus allowing for the unambiguous discrimination of individual DNA strands (see Figure 2 for examples). We then drew parallel lines on the enlargement and counted the number of DNA strands that crossed the reference lines per μm. The square of this value was the DNA density in this area of the network. Using this method, we measured the DNA density in several areas of Form I networks. In 10 measurements on five random networks, the standard deviation of these DNA densities was only 10% of the

Table I. Measurements of the minicircle density and the surface area of networks at different stages of replication

Network type	No. of networks measured	Minicircle planar density (minicircles/mm^2)	Network area (mm^2)
Form I	10	36 ± 4	137 ± 10
Replicating (central zone)	6	35 ± 5	139 ± 18
Replicating (peripheral zone)	6	77 ± 9	
Form II	10	64 ± 17 (38–90)	166 ± 52 (114–252)

mean (400 ± 40 strand intersections^2/μm^2). Furthermore, when EM showed clearly that a Form I network was folded over, the DNA density in the region of double thickness (780 ± 50 strand intersections^2/μm^2) was twice that of regions of single thickness (Figure 2A and B). Therefore, our measure of planar density has satisfactory precision and accuracy. Henceforth, we convert all planar densities into the more informative unit of minicircles/μm^2 by using the known density of Form I networks of 36 minicircles/μm^2 (5000 minicircles/137 μm^2 for a Form I network).

The planar density of replicated Form II networks was strikingly different from that of Form I networks (Figure 2C and D; Table I). Instead of the unique density observed with Form I networks, there is a large variation from one Form II network to another. In the 10 networks measured, the densities ranged from a value that was, within error, the same as the Form I networks to a little more than twice this value (range 34–90 minicircles/μm^2). The mean is 64 minicircles/μm^2 in the 10 networks measured. Figure 2C and D shows enlargements of regions of Form II networks with measured DNA densities of 34 and 69 minicircles/μm^2 respectively. DNA density measurements in different regions of a given Form II network did not reveal an internal variation significantly different from that of Form I networks. Therefore we propose that the valence of the Form II networks changes with time, and this causes the variation in minicircle density. This change can only be made by topoisomerases, which must act quickly compared with the time scale of remodeling of Form II networks because individual Form II networks are relatively uniform in density. The measurements of network area and valence presented below are fully consistent with these conclusions.

Determining the density of replicating networks presented an additional complication. We wished to measure the DNA density in the central prereplicative zone and the peripheral replicative zone separately. However, these zones cannot be distinguished by the EM technique used thus far because the nicked and gapped peripheral rings do not differ in appearance from the covalently closed central rings. The zones can be distinguished if the DNA is spread for microscopy in the presence of an intercalating dye (ethidium bromide), which supercoils the covalently closed minicircles in the central region but not the interrupted minicircles in the peripheral region. However, addition of the dye preferentially shrinks the covalently closed minicircles in the central region of the network (Rauch *et al.*, 1993) and makes it impossible to assess directly the relative DNA densities in the two zones. We avoided these problems as follows. First we visualized the networks in the presence of several low concentrations of ethidium bromide. We found that at 1 μg/ml of dye, the nicked peripheral region was not changed perceptibly yet the central zone was supercoiled enough to distinguish the two zones. Figure 3 shows examples of electron micrographs of a replicating network in the presence of ethidium bromide, and demonstrates that the zones can be distinguished. For the measurement of the density of the central region, the replicating networks were spread in the absence of dye, and only the innermost quarter of the network was analyzed.

For each network, four regions from the central and peripheral zones were measured. Figure 2E and F shows enlargements of the central and peripheral regions, respectively, of a replicating network. The density in the peripheral region doubles but the density of the prereplicative region is unchanged. For the six networks examined, the density in the peripheral region was 77 ± 9 minicircles/μm^2; in the central region it was 35 ± 5 minicircles/μm^2 (Table I). Thus, the central zone has the density of Form I networks, and the replicating region has about twice this density.

The surface area of isolated kDNA networks

The changes in Form II minicircle density during the G_2 phase reflect the changes in the underlying valence of the network (see below). The network surface area should also be dependent on minicircle valence. For a fixed number of minicircles, the area should decrease as the valence increases. Therefore we measured the surface areas of networks at each stage of replication, and histograms of the results are displayed in Figure 4. As shown in Figure 4A, the areas of 10 different Form I networks are quite uniform (137 ± 10 μm^2). Replicating networks, despite their increasing number of minicircles, also have a relatively uniform surface area; the mean is the same as that of Form I networks (Figure 4B, 139 ± 18 μm^2). In contrast, there is considerable variation in the surface areas of the 15 Form II networks measured; they ranged from 114 to 252 μm^2 (Figure 4C), with a mean of 166 μm^2. Surface areas varied from an area slightly less than that of a Form I network to nearly twice that value.

Although the measurements of density and area were made independently, the product of density and area for each Form II network should equal the total number of minicircles in the Form II network. This prediction is verified by the data in Figure 5, which show a linear relationship between network area and the reciprocal of network density. The slope of this line is the number of minicircles in a Form II network; the value obtained (10 000) is exactly that predicted. Our interpretation is that although Form II networks have a constant number of minicircles (twice Form I), the area of isolated networks gradually increases with time because of the continual drop in network valence to that of a Form I network.

Determination of the average minicircle valence in Form II networks

Previously we developed a method for determining the mean valence of a network (Chen *et al.*, 1995). In that study we partially digested Form I networks with a

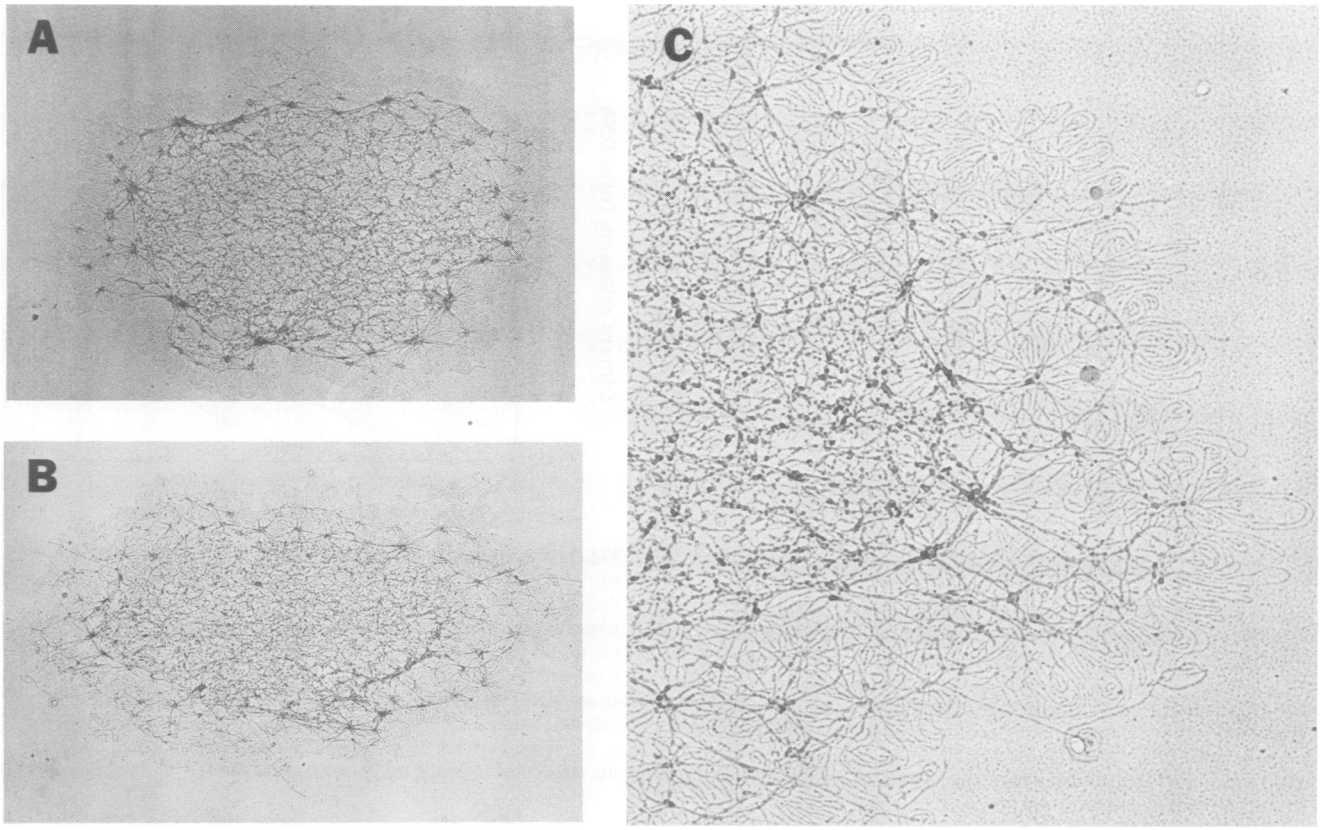

Fig. 3. Electron micrographs of replicating kDNA networks spread in the presence of ethidium bromide. The addition of 1 μg/ml ethidium bromide causes positive supercoiling in the central zone of covalently closed minicircles, but not in the peripheral zone of interrupted minicircles. As a result, the zones are easily distinguished. The network in (**A**) is at an early stage of replication, so almost all the DNA in the network is supercoiled. The replicated rings extend around the edge of the network. The network in (**B**) is at a later stage of replication. (**C**) shows a portion of the network in (B) at a 5-fold magnification.

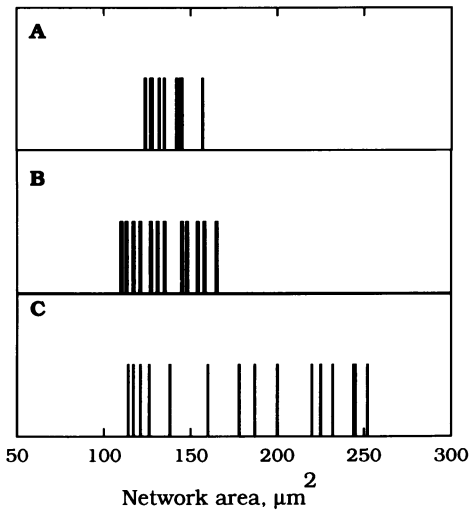

Fig. 4. Surface area of kDNA networks. The surface area of networks at three stages of replication was measured by EM. Each vertical line in the histograms represents an individual network. (**A**) Areas of 10 Form I networks; (**B**) areas of 14 replicating networks; (**C**) areas of 15 Form II networks.

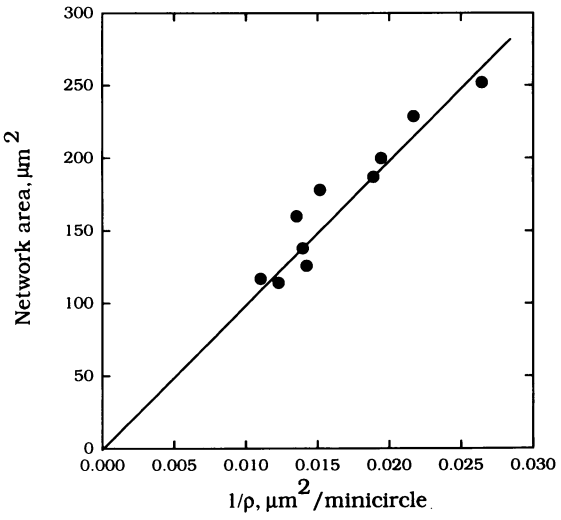

Fig. 5. Relationship between surface area and minicircle density of Form II networks. The area (A) and planar density (ρ) of 10 Form II networks was measured. $N = A\rho$, where N is the number of minicircles in the network. Therefore, A should be linearly related to ρ^{-1}, with the slope of the line equal to N.

restriction enzyme, *Xho*I, that cleaves essentially all minicircles once. We then measured the frequency of release of monomers, catenated dimers and catenated trimers. From a comparison of the results with those predicted from the random digestion of model networks, we concluded that the valence was 3.

We performed a similar experiment with the population of Form II networks. We first measured the release

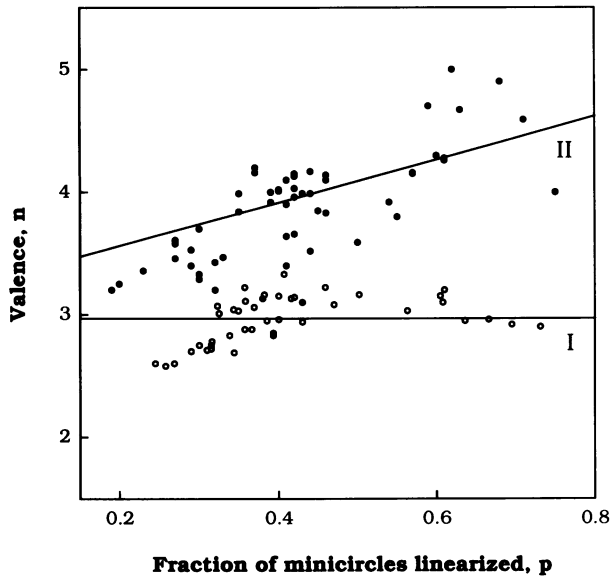

Fig. 6. Determination of the average valence of Form II networks from the fractional release of monomer minicircles. Form II kDNA networks were partially digested to the extent shown (p). The plotted values of the valence, n, were computed from the relationship $n = [\log (mon) - \log N - \log q]/\log p$, where mon is the number of monomer circles released, N is the total number of circles in the network and q is the surviving fraction of circles (Chen *et al.*, 1995). The results of 62 independent digestions of Form II networks are shown (●). For comparison, the results of digestion of Form I networks from our previous work (Chen *et al.*, 1995) are also indicated (○). The line labeled II is the calculated result with a 1:2 mixture of $n = 3$ (Figure 1A) and $n = 6$ (Figure 1C) networks. This mixture was chosen as the one whose calculated curve bisected the Form II data points. The line marked I is the horizontal line with a valence equal to the mean (2.94) of the Form I data points.

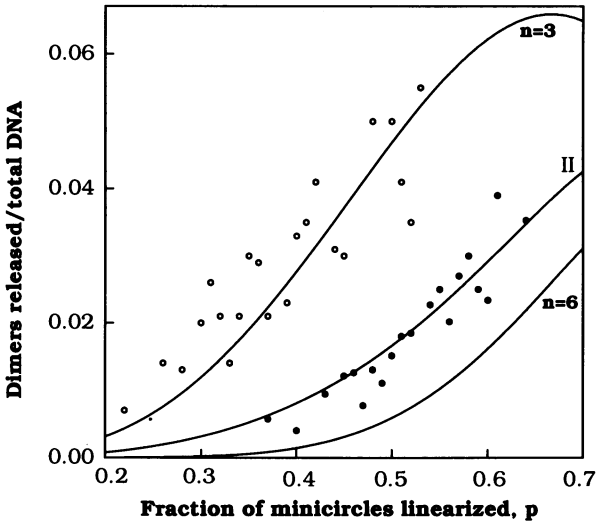

Fig. 7. The fraction of catenated dimers released as a function of the partial digestion of Form II kDNA networks. The amount of catenated dimers released as a function of linearization, p, of the network was measured by high-resolution agarose gel electrophoresis. Shown are the results (●) of 22 independent experiments. For comparison, the results of digestion of Form I networks from our previous work (Chen *et al.*, 1995) are also indicated (○). The line marked II is the calculated frequency assuming a 1:2 ratio of $n = 3$ (Figure 1A) and $n = 6$ (Figure 1C) networks. The lines marked $n = 3$ and $n = 6$ are the theoretical lines for the networks in Figure 1A and C, respectively.

of minicircle monomers and linearized minicircles as a function of the extent of digestion with *Xho*I. Using the formula in the legend to Figure 6, we then calculated the valence implied by each experiment. The results of 62 independent experiments are shown in Figure 6 (●). For a univalent network, the data should be distributed about a horizontal line whose y value equals the valence. This is what we obtained previously for the Form I network (Chen *et al.*, 1995), and the data are reproduced in Figure 6 for comparison (○). For the Form I networks, valence $(n) = 2.94 \pm 0.19$. It is clear that the mean valence of a Form II network is higher than that of a Form I network, and that the Form II networks have a range of valences. A substantial variation in valence will give the observed positive slope to the data points. This is because the networks with a lower valence will contribute relatively more intact monomers at the lower extents of digestion, leaving a greater contribution of the higher valence networks later in the reaction. Line II in Figure 6 is the theoretical curve for a mixture of networks having valences of 3 and 6, respectively, that bisects the data points. This is a first-order approximation for what we consider to be the actual population of Form II networks, which are continuously reduced in the G_2 phase to an endpoint valence of 3.

We next measured by high-resolution gel electrophoresis the amount of catenated dimers released by the digestion of Form II networks with *Xho*I (Figure 7). For comparison, we show the Form I data from our previous study ($n = 3$) and the theoretical curves for valences of 3 and 6 (Chen *et al.*, 1995). Once again, the Form II data are very different from that of Form I; there is no overlap of the data points. The solid line labeled II was calculated using the same approximation of a mixture of valence 3 and 6 networks, as in Figure 6. The fit is good. In conclusion, direct measurements of the valence of Form II networks show that, on average, the valence is clearly higher than that of Form I networks and is consistent with a mixture of networks with minicircle valences ranging between 3 and 6. Such a mixture would also explain the surface area and density measurements of Form II networks.

Discussion

We reported previously that minicircles in a *C.fasciculata* Form I network have an average valence of 3 and are probably arranged in a hexagonal array as shown in Figure 1A (Chen *et al.*, 1995). We suggested that this structure is established by constraining 5000 relaxed minicircles within the volume of a disk 1 μm in diameter—the size of the kinetoplast *in vivo*. We proposed that random topoisomerase action on minicircles at this concentration would produce a network of the observed valence under the conditions within the mitochondrion. Furthermore we suggested that the constraint at the disk perimeter might be the mitochondrial membrane, as electron micrographs of *C.fasciculata* thin sections usually show that the membrane abuts the edge of the kinetoplast disk (see, for example, Renger and Wolstenholme, 1972).

The Form I network is the mature resting state in which the minicircles are relaxed, covalently closed rings. Here we have examined two additional network states. One is the replicating form, which contains a central zone of non-replicated, covalently closed minicircles and a peri-

pheral zone of nicked or gapped newly replicated minicircles. The other state is where the peripheral zone grows at the expense of the central zone until the network doubles to the 10 000 ring Form II network.

We used three methods to analyze the structure of networks at different stages of replication. One method, described previously, allowed for the direct calculation of the mean minicircle valence from the frequency of linearized minicircles, minicircle monomers and catenated oligomers released from the network by partial restriction enzyme digestion (Chen *et al.*, 1995). The second method, described here for the first time, revealed the density of minicircles within a region of the planar network by measurements from electron micrographs. The minicircle density increases with network valence. The third method involved measuring the network surface area on electron micrographs. This quantity is inversely related to valence. The first method is the most direct but its power is limited with heterogeneous populations of networks.

The data from all three methods agree completely and led us to a detailed model of the topological changes that occur during kDNA replication. The model is strikingly different from the most parsimonious scheme in which the action of topoisomerases is limited to the removal of covalently closed minicircles from the central region of the network and the reattachment of the interrupted daughters to the network periphery with the same topology as in the prereplicative form. Instead, we found that the topology of the network is readjusted continuously during the replication and maturation of Form II networks.

We found that the valence of the replicated region of S phase networks was increased, as shown by the measurement of planar minicircle density. In prereplication Form I networks, the density was 36 minicircles/μm^2. In the peripheral zone of replicating networks, the density was about twice as high—77 minicircles/μm^2. We adopt the valence of the peripheral zone as 6 for the rest of this discussion. This is a reasonable value given the doubling of density, but the valence of this zone was not determined directly. The structure of different Form II networks was surprisingly heterogeneous, with minicircle density ranging from ~34 to 90 minicircles/μm^2 and area from 114 to 252 μm^2. Direct valence measurements of Form II networks, shown in Figures 6 and 7, also indicated a mixture of valences, probably between 3 and 6. Despite the difference in valence among individual Form II networks, the valence within any network was uniform, as indicated by the density measurements.

A scheme that explains these data is shown in Figure 8. Form I networks have 5000 minicircles with a valence of 3. When replication begins during the S phase, minicircles are released from the network and, after replication, the nicked or gapped progeny minicircles are attached around the network periphery. The newly attached minicircles at the peripheral region have twice the density, and the surface area of the replicating network does not grow relative to that of a Form I network. The densities of the central zones of the replicating networks remain the same during the S phase. Presumably the network is prevented from increasing in area, possibly by the mitochondrial membrane. Therefore the newly replicated minicircles are packed at the higher density. Even when the network has finished replication and contains 10 000 minicircles, it is

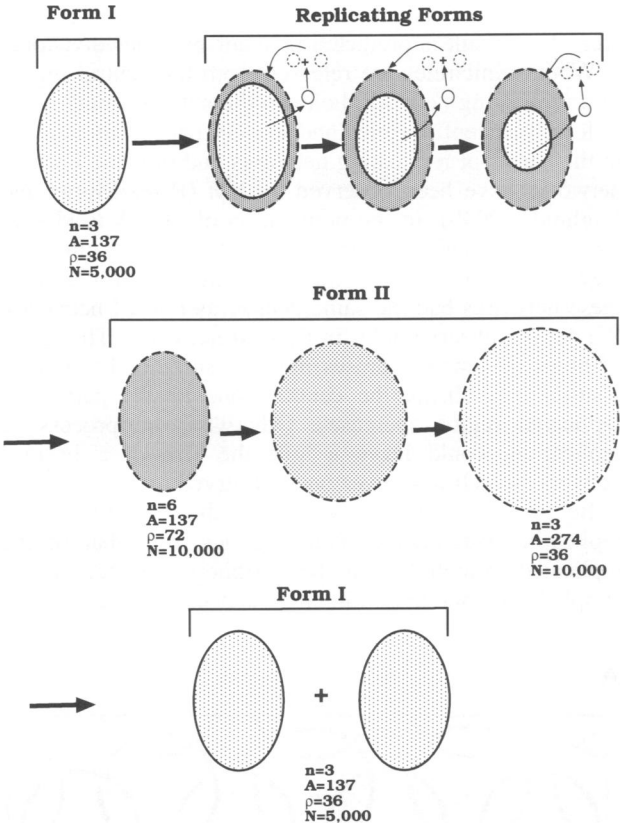

Fig. 8. Model for the replication of kDNA networks. The ovals symbolize kDNA networks at the prereplicative (Form I), replicating and postreplicative (Form II) stages. The ovals enclosed by a solid line contain covalently closed minicircles; those enclosed by a dashed line contain interrupted minicircles. The networks are characterized by these measured values: valence (n), surface area (A), planar density (ρ) and the number of minicircles (N). The density of dots in the oval shows the minicircle density; the size of the oval represents the area of the network. Small circles represent free minicircles, either covalently closed or with gaps (interrupted line).

still constrained in this limited space. Therefore, the surface area of the isolated network has still not increased and we infer that a nascent Form II network has a minicircle valence of 6. So, during the G_2 phase of the cell cycle there must be a gradual increase in space available to the network, possibly by expansion of the mitochondrial membrane. The random action by topoisomerases results in a gradual enlargement of the network surface area and a drop in valence to 3. To account for the uniform valence of any given Form II network, topoisomerase action must be fast relative to the time of remodeling.

Pérez-Morga and Englund (1993b) concluded that the interruptions in the Form II network minicircles must be repaired before network division. This conclusion was based on the observation that mosaic networks, those containing interrupted and repaired minicircles, were always double sized rather than single sized. We draw the same conclusion from different experiments. We did not observe Form II networks with the density and area of Form I networks, which is the predicted structure of the key intermediate if network division preceded repair. Instead, the Form II networks with the area of Form I networks had twice their density, and the Form II networks

with the same density of Form I networks had twice their area. This result is predicted if repair precedes division.

When minicircles are released from the central region of a replicating network, holes in the network must form, at least transiently. Holes and loosely packed minicircles in the center of replicating networks and in some Form II networks have been observed by EM (Pérez-Morga and Englund, 1993b). In the preparation of kDNA used here there were small holes in only ~20% of the replicating networks. Otherwise, we found that the central region of these networks had the same density as Form I networks. We did not observe holes in Form II networks. The repair of holes by topoisomerases must be sufficiently rapid to continuously shrink the central zone as the peripheral replicated region increases. Otherwise the process of replication would leave a hole the size of a Form I network, which has never been observed.

Because the minicircle valence in the central region of replicating networks remains distinct from that of the replicated minicircles on the periphery, valence cannot simply be a function of minicircle concentration at equilibrium. If it were, the two zones would have the same valence. Because the interruption in the replicated rings should not greatly change the physical properties of the DNA (Vologodskii, 1992), it is highly unlikely that the valence difference in the two zones is simply caused by the interruptions. Perhaps a marking protein, which enables topoisomerases to distinguish interrupted from covalently closed rings, changes the equilibrium to the high valence form. The removal of these proteins, after network remodeling is completed in the G_2 phase, could permit repair of the interruptions in the minicircles which in turn could signal network division.

Although the model in Figure 8 explains all of our results, it needs further verification. The absence of growth in the surface area of the isolated network during replication in our study contrasts with measurements of the size of the kinetoplast disk *in situ* by fluorescence microscopy of 4′,6-diamidino-2-phenylindole-stained cells (Ferguson *et al.*, 1992). In that study, kinetoplast disks undergoing replication were intermediate in area between pre- and postreplicative forms. It is possible that this difference

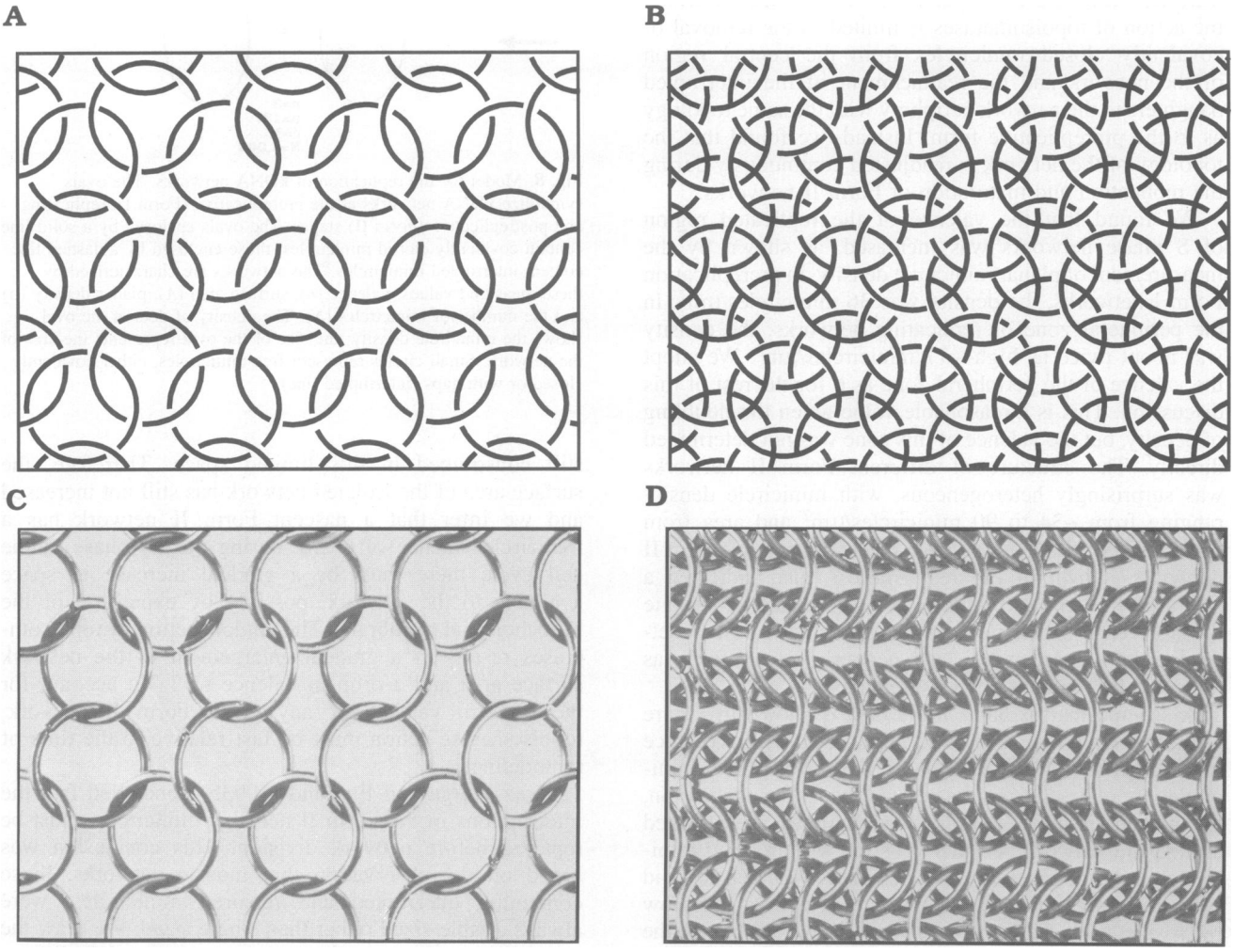

Fig. 9. Models for the *C.fasciculata* kDNA networks. (**A** and **B**) Planar projections. Each circle represents a kDNA minicircle; at an intersection the underpassing circle is interrupted. (A) Diagram of a Form I network scaled to the area of the isolated Form I networks. The valence is 3 and the tiling is hexagonal. (B) Diagram of a Form II network scaled to 4/3 the area of the isolated nascent Form II network. It was not scaled to the isolated network so that the minicircles could be more easily discerned. Note that the linking of a ring to each of its six neighboring rings converts pattern A to B and vice versa. (**C** and **D**) Chain mail models of the kDNA network. Each metal ring represents a minicircle. (C) A Form I model to the scale of the isolated network. (D) A nascent Form II model to the scale of the isolated network.

from our study results from the method of preparation of cells for fluorescence microscopy, which included treatment with protease and SDS to reorientate the kinetoplast disk. Thus the disk area *in situ* could have changed because of a release of a subset of the proteins that maintain its shape.

One previous EM study of *Trypanosoma brucei* kDNA networks at different stages of replication revealed similarities to our observations. As with *C.fasciculata*, replicating networks did not grow in surface area relative to Form I networks, and there was an expansion in surface area only after doubling of the minicircle copy number (Hoeijmakers and Weijers, 1980). However, another EM study using a different strain of *T.brucei* indicated a gradual expansion of the network during replication (Ferguson *et al.*, 1994). Further work is needed to resolve these differences.

The topological data for *C.fasciculata* that we obtained suggest physical structures for valence 3 and 6 networks. Valence 3 networks have been discussed previously and are presented here for comparison (Chen *et al.*, 1995). Figure 9A and B shows valence 3 and 6 network structures in simplified planar diagrams so that the underlying organization is easy to observe. Each minicircle is represented by a ring linked to three and six neighbors, and the tiles are hexagons and triangles, respectively. This is the only reasonable tiling pattern for a regular valence 6 network. Despite the striking differences between these networks, the valence 6 network can be derived simply from the valence 3 network by linking a minicircle in the center of the hexagonal tile to each of the six surrounding minicircles. This could be the basic process for generating Form II networks from Form I networks during replication. The reverse process of generating valence 3 networks from valence 6 networks could be the way Form II networks are matured.

The packing of the DNA in the networks can be better appreciated by constructing 3-D models. A convenient material is chain mail, as used in medieval armor. The individual links of the mail represent the minicircles. Chain mail with valences of 3 and 6 are shown in Figure 9C and D, respectively. Both model networks pleat readily so that the rings in one row tilt in the opposite direction to the rings in the neighboring rows. The result is surprisingly flexible structures. When these model networks are extended maximally, the valence 6 model (Figure 9D) approximates to the planar density of nascent Form II networks, and the valence 3 model (Figure 9C) approximates to the planar density of the mature Form II networks.

Materials and methods

Isolation of kDNA

Crithidia fasciculata was grown to mid-log phase at room temperature in brain heart infusion medium supplemented with 20 μg/ml hemin. kDNA was isolated as described previously (Hajduk *et al.*, 1984), except that the sarkosyl lysate was digested with RNase A (200 U/ml) and RNase T1 (0.2 mg/ml) for 90 min at 37°C prior to centrifugation in a CsCl step gradient. Networks at different stages of replication were fractionated by CsCl–propidium diiodide equilibrium centrifugation (Englund, 1978; Rauch *et al.*, 1993).

Enzyme reactions

The partial digestion of isolated kDNA networks by the restriction enzyme *Xho*I was performed as described previously (Rauch *et al.*, 1993).

Fractionation of network fragments by gel electrophoresis

Two electrophoresis systems were used as described previously (Chen *et al.*, 1995). For the optimal separation of catenated oligomers, digests were separated by high-resolution electrophoresis (Sundin and Varshavsky, 1980). For the optimal resolution of monomer minicircles from linearized minicircles, electrophoresis was through a standard TBE agarose gel.

Electron microscopy

kDNA was prepared for microscopy using the standard formamide method described by Davis *et al.* (1971). Some samples were treated with ethidium bromide at the concentration of 1 μg/ml to distinguish nicked from closed minicircles before spreading (Englund, 1978; Hoeijmakers and Weijers, 1980). Samples on parlodion-coated copper grids were stained with uranyl acetate, rotary shadowcast with Pt/Pd and viewed in a JEOL 100B electron microscope.

Determination of minicircle valence

We determined the valence of the kDNA network from two independent sets of data (Chen *et al.*, 1995). We first measured with TBE gels the fractional release of minicircle monomers and linearized minicircles as a function of the extent of *Xho*I digestion. Using the formula in the legend to Figure 6, we then calculated the valence. Second, high-resolution gel electrophoresis was used to measure the release of catenated dimers as a function of the extent of network digestion with *Xho*I. We then interpreted these results by comparing them with theoretical curves for dimer release from the model networks with valences of 3 and 6, as shown in Figure 7.

Acknowledgements

We thank Hal Heydt from the Society for Creative Anachronism for the construction of the chain mail models of the kDNA networks. This work was supported by grants from NIH (GM31657) and NSF (DMS-8820208) to N.R.C., and from the MacArthur Foundation and NIH (GM27608) to P.T.E.

References

Benne,R. (1994) *Eur. J. Biochem.*, **221**, 9–23.
Chen,J., Rauch,C.A., White,J.H., Englund,P.T. and Cozzarelli,N.R. (1995) *Cell*, **80**, 61–69.
Cozzarelli,N.R. (1993) *Harvey Lectures*, **87**, 35–55.
Davis,R.W., Simon,M. and Davidson,N. (1971) *Methods Enzymol.*, **21D**, 413–428.
Englund,P.T. (1978) *Cell*, **14**, 157–168.
Ferguson,M., Torri,A.F., Ward,D.C. and Englund,P.T. (1992) *Cell*, **70**, 621–629.
Ferguson,M.F., Torri,A.F., Pérez-Morga,D., Ward,D.C. and Englund,P.T. (1994) *J. Cell Biol.*, **126**, 631–639.
Hajduk,S.L., Klein,V.A. and Englund,P.T. (1984) *Cell*, **36**, 483–492.
Hajduk,S.L., Harris,M.E. and Pollard,V.W. (1993) *FASEB J.*, **7**, 54–63.
Hoeijmakers,J.H.J. and Weijers,P.J. (1980) *Plasmid*, **4**, 97–116.
Melendy,T., Sheline,C. and Ray,D.S. (1988) *Cell*, **55**, 1083–1088.
Pérez-Morga,D. and Englund,P.T. (1993a) *Cell*, **74**, 703–711.
Pérez-Morga,D. and Englund,P.T. (1993b) *J. Cell Biol.*, **123**, 1069–1079.
Rauch,C.A., Pérez-Morga,D., Cozzarelli,N.R. and Englund,P.T. (1993) *EMBO J.*, **12**, 403–411.
Ray,D.S. (1987) *Plasmid*, **17**, 177–190.
Renger,H.C. and Wolstenholme,D.R. (1972) *J. Cell Biol.*, **54**, 346–364.
Shapiro,T.A. and Englund,P.T. (1995) *Annu. Rev. Microbiol.*, **49**, 117–143.
Shlomai,J. (1994) *Parasitol. Today*, **10**, 341–346.
Simpson,A.M. and Simpson,L. (1976) *J. Protozool.*, **23**, 583–587.
Simpson,L. (1987) *Annu. Rev. Microbiol.*, **41**, 363–382.
Simpson,L. and Maslov,D.A. (1994) *Science*, **264**, 1870–1871.
Stuart,K. and Feagin,J.E. (1992) *Int. Rev. Cytol.*, **141**, 65–88.
Sugisaki,H. and Ray,D.S. (1987) *Mol. Biochem. Parasitol.*, **23**, 253–263.
Sundin,O. and Varshavsky,A. (1980) *Cell*, **21**, 103–114.
Vologodskii,A. (1992) In Vologodskii,A. (ed.), *Topology and Physics of Circular DNA*. Academic Press, New York, NY, pp. 8–28.

Received on May 25, 1995; revised on July 13, 1995